14th International Conference on Structural Safety and Reliability - ICOSSAR'25
1-6 June, 2025 - Los Angeles California, USA
R. Ghanem, E. Johnson, S. Masri and A. Olivier (Eds)

# BEYOND STATISTICAL FITTING: IMPROVING RELIABILITY ANALYSIS THROUGH PHYSICALLY CONSISTENT BRIDGE TRAFFIC LOAD MODEL

**AKBAR RIZQIANSYAH[1], COLIN C. CAPRANI[2]**

[1] Department of Civil Engineering, Monash University
Melbourne, Australia
akbar.rizqiansyah@monash.edu

[2] Department of Civil Engineering, Monash University
Melbourne, Australia
colin.caprani@monash.edu

**Key words:** structural reliability, reliability analysis, bridge traffic loading, upper bound, extreme value, Bayesian

**Abstract.** The estimation of lifetime bridge traffic loading is important for ensuring safety. This is commonly achieved by fitting extreme value distributions, where the distribution type dictates the upper tail behavior: unbounded (Type I), heavy-tailed (Type II), or upper-bounded (Type III). The correct modeling of the upper tail is crucial, as this is where loading more likely exceeds resistance, leading to collapse. However, many studies overlook the influence of the underlying physical processes on the upper tail behavior. This research investigates how the physical bounds of traffic loading affect the resulting extreme distribution type and its applications to reliability analysis. First, we examine the effects of naturally upper-bounded and truncated systems on the resulting extreme value distribution. The resulting block maxima probability density converges to the upper-bounded extreme value distribution, even when the original distribution is heavy-tailed. Second, we propose Bayesian modeling to integrate knowledge about traffic, such as axle configurations and mass limits, into the statistical model. Hamiltonian Monte Carlo No-U-Turn Sampler (HMC NUTS) is used to estimate the upper bound of traffic. Finally, we compare the physically informed (upper-bounded) model with the uninformed (unbounded) model in bridge reliability analysis. We show that the physically informed model reduces the probability of failure over the common range of the parameter space. These findings highlight the necessity of selecting appropriate extreme value distribution types based on physical processes to enhance safety and reliability analysis.

## 1 INTRODUCTION

The statistical modeling of bridge traffic (live) load has wide applications and, consequently, has received much attention from numerous studies. Most design codes derive their live load model from the live load return level (e.g., the 100-year live load return level) [1]. Recent works on the calibration of design codes utilize reliability analysis, which requires the characterization of the statistical distribution of the live load (e.g., [2, 3]). Higher tier probability-based bridge assessment also utilizes reliability assessment, and requires the statistical distribution of site-specific traffic load to obtain a more accurate reliability index than conventional methods [4].

Commonly, extreme value theory is used as the basis for the statistical model of live load [1]. Specifically, the block maxima method leads to the choice of the Generalized Extreme Value (GEV) distribution to fit periodic maxima (e.g., daily, monthly, or yearly maxima) of traffic load (for example, [5, 6]). Further developments have been proposed to expand on the GEV distribution specific to bridge traffic loading. For example, modeling multi-vehicle presence [7]; multi-modalities [8]; modeling across a road network [9]; incorporating traffic growth [10], among others.

However, most studies for bridge traffic loading still propose distributions with unbounded upper tails, neglecting the fact that traffic is a physical process that is upper-bounded by physical limitations. This includes studies using the GEV distribution with shape parameter estimates larger than or equal to zero, suggesting unbounded Gumbel or Fréchet tails (type I and II GEV, respectively). The Gumbel tail is also commonly used for the bridge traffic load distribution in reliability analysis [11]. This leads to a non-zero probability of traffic loading that is beyond what is physically possible.

This work shows that traffic must be upper-bounded and follows the Weibull domain of attraction of the GEV distribution with shape parameter $\xi < 0$. A method to estimate the traffic load upper bound is proposed, along with a method to incorporate information about the upper bound (e.g., the system's physical limits) to improve the estimations. Finally, the implications of choosing a physically consistent upper-bounded live load model are explored within the reliability analysis framework.

## 2 METHODOLOGY

### 2.1 Extreme Value Theory

The block maxima approach of extreme value theory is frequently used to model the block maxima (e.g., daily, monthly, or yearly maxima) of bridge traffic load distribution [1]. In summary, given a sequence of independent and identically distributed random variables (i.e., traffic loading) $\{S_1, ..., S_N\}$, the distribution of the block maxima (i.e., extreme traffic loading) $X = \max\{S_1, ..., S_N\}$ converges to the Generalized Extreme Value (GEV) distribution with the probability and cumulative distribution function ($g$ and $G$, respectively) [12]:

$$g(x|\mu, \sigma, \xi) = \frac{1}{\sigma} t(x)^{\xi+1} \exp(-t(x)), \tag{1}$$

$$G(x|\mu, \sigma, \xi) = \exp(-t(x)), \tag{2}$$

where $\mu$, $\sigma$, and $\xi$ are the location, scale, and shape parameters, respectively, and

$$t(x|\mu, \sigma, \xi) = \begin{cases} \left(1 + \xi \left(\frac{x-\mu}{\sigma}\right)\right)^{-1/\xi}, & \text{for } \xi \neq 0 \\ \exp\left(-\frac{x-\mu}{\sigma}\right), & \text{for } \xi = 0. \end{cases} \tag{3}$$

The shape parameter $\xi$ dictates the support and tail behavior of the distribution. $\xi = 0$ (Type I, Gumbel) has support along the real number line. $\xi > 0$ (Type II, Fréchet) is lower bounded with support $x \in [\mu - \sigma/\xi, +\infty)$. $\xi < 0$ (Type III, Weibull) is upper-bounded with support $x \in (-\infty, \mu - \sigma/\xi]$.

### 2.2 Upper-bounded GEV Distribution

For the strictly Weibull case ($\xi < 0$), the GEV distribution can be parameterized in terms of its mean ($\epsilon$), upper bound ($\zeta$), and shape parameter ($\xi$) with the cumulative distribution function as Eq.

(2) and the probability distribution function:

$$g(x|\epsilon,\zeta,\xi) = \frac{\xi'}{\xi(\epsilon-\zeta)} t(x|\epsilon,\zeta,\xi)^{\xi+1} \exp\left(-t(x|\epsilon,\zeta,\xi)\right), \tag{4}$$

where $\xi' = \Gamma(1-\xi)$, $\Gamma(\cdot)$ is the gamma function, and

$$t(x|\epsilon,\zeta,\xi) = \left(\frac{\xi'\left(\zeta - x\right)}{\zeta-\epsilon}\right)^{-1/\xi}, \tag{5}$$

The mean and the upper bound are related to the conventional $\mu, \sigma, \xi$ parameterization by

$$\epsilon = \mu - \sigma\left(1-\xi'\right)/\xi, \qquad \zeta = \mu - \sigma/\xi. \tag{6}$$

### 2.3 Bayesian Modeling

In this work, Bayesian modeling is used to infer the parameters of the GEV distribution. Bayesian modeling is underpinned by the use of Bayes' rule

$$P(\vec{\theta}|\vec{x}) = \frac{P(\vec{x}|\vec{\theta})P(\vec{\theta})}{\int P(\vec{x}|\vec{\theta})P(\vec{\theta})d\vec{\theta}}, \tag{7}$$

where $\vec{\theta}$ are the GEV parameters ($\{\mu,\sigma,\xi\}$, or $\{\epsilon,\zeta,\xi\}$), $\vec{x}$ is a vector of the observed values, $P(\vec{\theta}|\vec{x})$ is the posterior distribution (i.e., estimate) of the parameters $\vec{\theta}$, $P(\vec{x}|\vec{\theta})$ is the likelihood function

$$P(\vec{x}|\vec{\theta}) = \Pi_{i=1} g(x_i|\vec{\theta}), \tag{8}$$

$g(\cdot)$ is the GEV probability distribution function (Eqs. (1) or (4)), $P(\vec{\theta})$ is the prior distribution of $\vec{\theta}$, and $\int P(\vec{x}|\vec{\theta})P(\vec{\theta})d\vec{\theta}$ is the normalizing constant such that the posterior distribution integrates to 1 over the range of the $\vec{\theta}$ space. The normalizing constant is usually mathematically intractable. In this work, Hamiltonian Monte Carlo No-U-Turn sampler, as implemented in the *pymc* package, is used to sample the posterior distribution directly [13, 14].

## 3 BOUNDED PHYSICAL PHENOMENON

### 3.1 The Upper-boundedness of Bridge Traffic Loading

Bridge traffic loading is a physical phenomenon that is bounded by both physical and non-physical constraints. Physical limits include material (e.g., the strength of axles), geometric (e.g., limits on the maximum volume of cargo), mechanical (e.g., the towing capacity of prime movers), etc. Non-physical limits include economic (e.g., the maximum cargo based on the available cargo demand; see [15, 16, 17] for studies in Australia) and regulations (e.g., allowable axle configurations for heavy vehicles, and enforcement of gross vehicle weight). All traffic loadings are bounded by the above limits, which are finite. Therefore, traffic loading is finite and is upper-bounded. Figure 1 illustrates the relative location of the physical upper bound, the traffic upper bound, and the observed traffic loads.

It is common to assume that the extremes of bridge traffic loading sufficiently converge to the GEV distribution [1] (i.e., fulfill the conditions for convergence under extreme value theory [12]). It

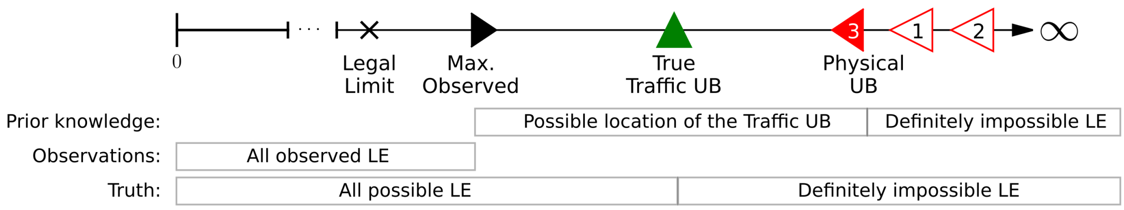


**Figure 1**: The location of the physical upper bound (UB) and the true traffic load upper bound. The different physical upper bounds (labeled 1, 2, 3) are due to different physical limitations, e.g., geometric and mechanical limits. Other (non-physical) limitations may govern, which are below or at least equal to the physical upper bound. The smallest of all of the limitations (both physical and non-physical) is the true traffic upper bound. Note that the true traffic bound is unknown.

is known that upper-bounded distributions converge to the Weibull domain of attraction [18]. It could thus be concluded that traffic loading converges to the GEV distribution with $\xi < 0$, and the Gumbel and Fréchet domain of attraction ($\xi \geq 0$) is not possible.

However, some studies have suggested heavy-tail behavior in traffic loading (e.g., [19, 5]). It can be hypothesized that traffic is heavy-tailed, but upper-bounded by physical and non-physical limits via a truncation process. An example of a truncation process is gross weight enforcement, where traffic loading beyond some legal limit is effectively censored and impossible to observe. However, in this case, we show in Section 3.2 that traffic loading still belongs to the Weibull domain of attraction.

### 3.2 Extremes of Truncated Random Variables

Let $X$ be a truncated distribution with an upper truncation point $b$. The probability and cumulative distribution function ($f$ and $F$) are

$$f(x) = \begin{cases} h(x)/H(b), & \text{for } x \leq b \\ 0, & \text{otherwise} \end{cases} \tag{9}$$

$$F(x) = H(x)/H(b), \tag{10}$$

where $h(x)$ and $H(x)$ are the probability and the cumulative distribution function of the non-truncated distribution.

Von Mises provides sufficient conditions for a random variable $X$ with distribution function $F$ to belong to the Weibull domain of attraction [20]. Denote $\omega(F)$ as the upper support of $F$, then $X$ is in the Weibull domain of attraction if

$$\omega(F) < \infty \text{ and } \lim_{x \to \omega(F)} (\omega(F) - x) \frac{f(x)}{1 - F(x)} = \alpha \tag{11}$$

for some $\alpha > 0$. Note that $\alpha = -1/\xi$, where $\xi$ is the GEV shape parameter (Eqs. (1) and (4)) [20]. We can show that an upper-truncated distribution belongs to the Weibull domain of attraction with $\xi = -1$, regardless of the initial non-truncated distribution.

**Theorem 3.1.** *Let $Y$ be a random variable with distribution function $H$ and a lower and upper support $a_y$ and $b_y$, respectively; $a_y < b_y \leq \infty$. Let $X$ be the random variable $Y$ truncated at $b$, and $a_y < b < b_y \leq \infty$. If the probability density function of $Y$ at $b$ is non-zero, then $X$ belongs in the Weibull domain of attraction and $\lim_{N \to \infty} F(x) = G(x)$ where $F$ is the distribution function of $X$ and $G$ is the GEV distribution function with shape parameter $\xi = -1$.*

*Proof.* For an upper truncation at $b < \infty$, then $\omega(F) = b$. Thus, $\omega(F) < \infty$. The second sufficient condition for the Weibull domain of attraction (Eq. (11))

$$\lim_{x \to \omega(F)} (\omega(F) - x) \frac{f(x)}{1 - F(x)} = \lim_{x \to b} \frac{(b - x)h(x)}{H(b) - H(x)}. \tag{12}$$

Using l'Hôpital's rule:

$$\lim_{x \to b} \frac{(b - x)h(x)}{H(b) - H(x)} = \lim_{x \to b} 1 - \frac{(b - x)h'(x)}{h(x)}, \tag{13}$$

where $h'(x)$ is the derivative of $h(x)$. $h(b)$ is non-zero, thus $\lim_{x \to b} h'(x)/h(x)$ is a finite constant. Therefore,

$$\lim_{x \to b} 1 - \frac{(b - x)h'(x)}{h(x)} = 1, \tag{14}$$

and $\alpha = -1/\xi = 1$, thus $\xi = -1$. □

The above shows that for truncated random variables, their extremes converge to the Weibull domain of attraction. The case of a naturally bounded random process is already discussed in detail [18, 12]. Thus, naturally upper-bounded and upper-truncated processes must converge to the GEV distribution with $\xi < 0$, regardless of whether the original parent is heavy-tailed.

### 3.3 Distribution of Bridge Traffic Loading

A traffic micro-simulation for the midspan bending moment of a 20 m simply supported bridge is performed based on methodologies described in [21, 1]. The weights, spacing, and configurations of the vehicle axles are simulated based on traffic on the West Gate Bridge, Australia, with noise added following triangular distributions with a known upper bound. This imposes a traffic that has a known natural upper bound, against which the methodologies proposed in this work can be verified.

The GEV parameters are inferred using the Bayesian model (Section 2.3) and the conventional GEV distribution (Section 2.1) against observed daily, monthly, and yearly maxima (Figure 2). Note the Fréchet fit of the daily maximum bending moment, implying a non-zero probability of loads larger than the upper bound. This result is contrary to the upper-bounded nature of bridge traffic load. In contrast, the larger block maxima (monthly and yearly) correctly exhibit an upper-bounded tail.

Figure 3 shows a trend of the estimate of $\xi$ with changing block sizes. The green bands are estimates using the upper-bounded likelihood (and priors, as discussed later in Section 3.4). At small block sizes, the conventional GEV infer Fréchet tails ($\xi > 0$), despite the upper-boundedness of the traffic simulation. In contrast, the upper-bounded model (green band) correctly infers bounded distribution throughout all block sizes. As the block size increases, the estimate of $\xi$ using the two methods becomes similar. However, note that there is still a non-zero probability for $\xi > 0$ using the conventional model, resulting in a non-zero probability of an unbounded traffic load distribution.

### 3.4 Estimation of Traffic Load Upper Bound

We propose the use of the re-parameterized GEV distribution (Section 2.2) to estimate the upper bound of bridge traffic loading. Two important changes are made compared to the conventional model:

1. The likelihood function (Eq. (8)) uses the upper-bounded probability distribution function (Eq. (4)).

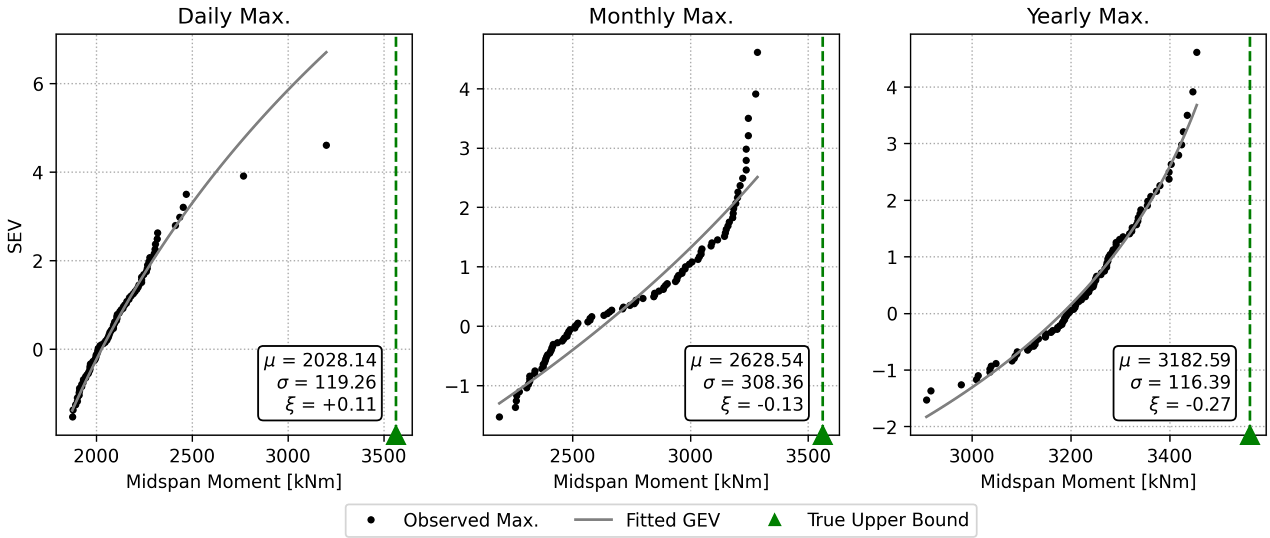


**Figure 2**: Observed maxima on the Gumbel Probability plot. The straight lines are the fitted GEV using Bayesian modeling to estimate the parameter posterior. The presented parameter estimate is the mode of the posterior distribution.

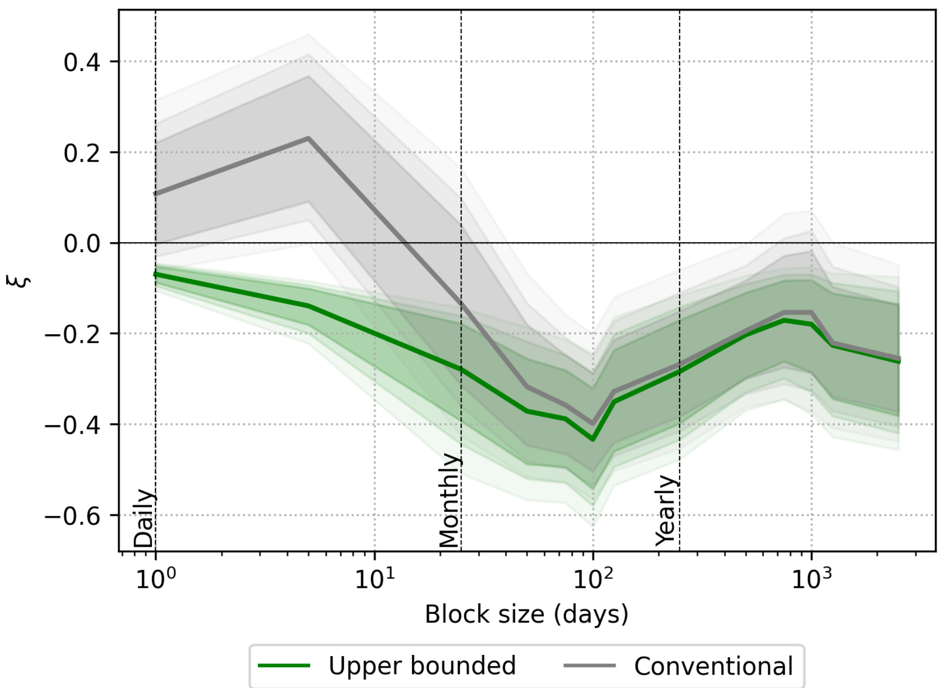


**Figure 3**: The estimated shape parameter ($\xi$) of bridge traffic load using the upper-bounded (green) and conventional (grey) parameterization. The solid line is the mode of the posterior distribution (point estimate). The bands are, in order of transparency, the 95%, 99%, and 99.9% posterior highest density interval.

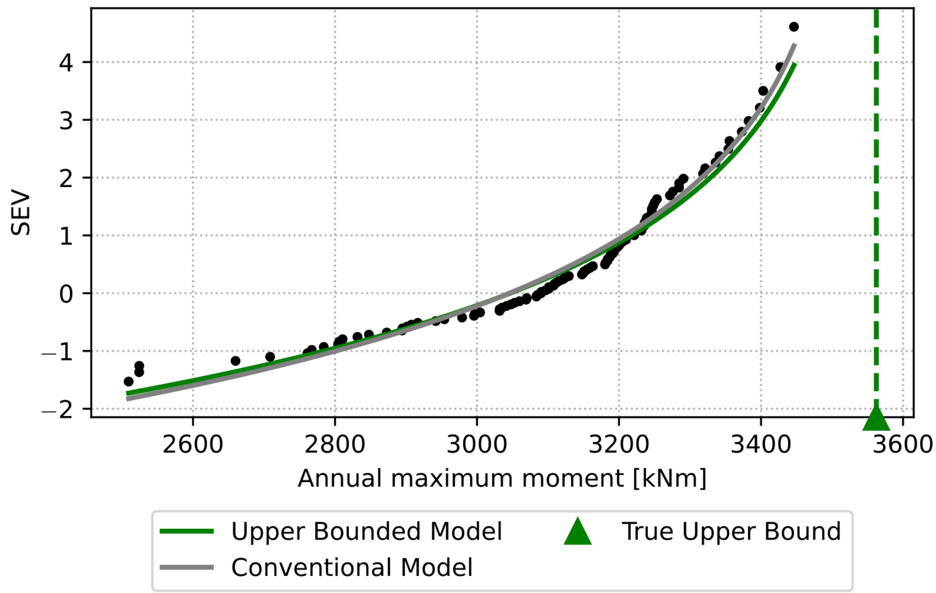


**Figure 4**: Upper bounded and conventional (unbounded GEV) fit to annual bridge traffic load.

2. The prior distribution ($P(\vec{\theta})$) applies a prior distribution on the upper bound ($\zeta$).

The prior for $\zeta$ in this work is a flat (uniform) prior between the maximum observed load effect and the physical upper bound, i.e., the range of possible locations of the traffic upper bound (Figure 1). The physical upper bound loading is a heavy load platform, with an axle spacing of 1.2 m, each with 500 kN, covering the whole bridge. The physical upper bound loading results in a midspan bending moment of 9615 kNm.

The resulting Bayesian fit on the annual maxima using the upper-bounded and conventional unbounded parameterization is similar, indicating that both methods mostly agree (Figure 4). However, the upper-bounded model can correctly estimate the traffic load upper bound ($\zeta$), while the conventional model is unable to estimate $\zeta$ as there is a non-zero probability that $\xi > 0$ in the conventional model (Figure 5). Figure 5 shows $\xi \neq -1$, indicating that traffic is not a truncated process, in line with this study's simulation (Section 3.3). This result shows how the proposed upper-bounded model, considering the physical bounds of traffic load, can estimate the traffic load upper bound and avoid physically impossible values.

# 4 RELIABILITY ANALYSIS

## 4.1 Limit State Function

A generic dimensionless limit state function is adopted after [22, 23], and applied in [3]

$$g(z) = \omega_R z R - \omega_S \left[(1 - a_q)\left(a_g G + (1 - a_g)P\right) + a_q Q\right], \tag{15}$$

where $\omega_R$, $\omega_S$, $R$, $G$, $P$, and $Q$ are dimensionless random variables (Table 1) with unit mean and standard deviation equal to their coefficient of variation; $a_g$ and $a_q$ are normalizing constants for the proportion of the self-weight to the overall dead load, and the proportion of the live load to the total load, respectively; $z$ is the *design solution*, obtained by solving the design Eq. (16)

$$\phi z R_k = (1 - a_q)\left[a_g \gamma_g G_k + (1 - a_g)\gamma_p P_k\right] + a_q \gamma_q Q_k, \tag{16}$$

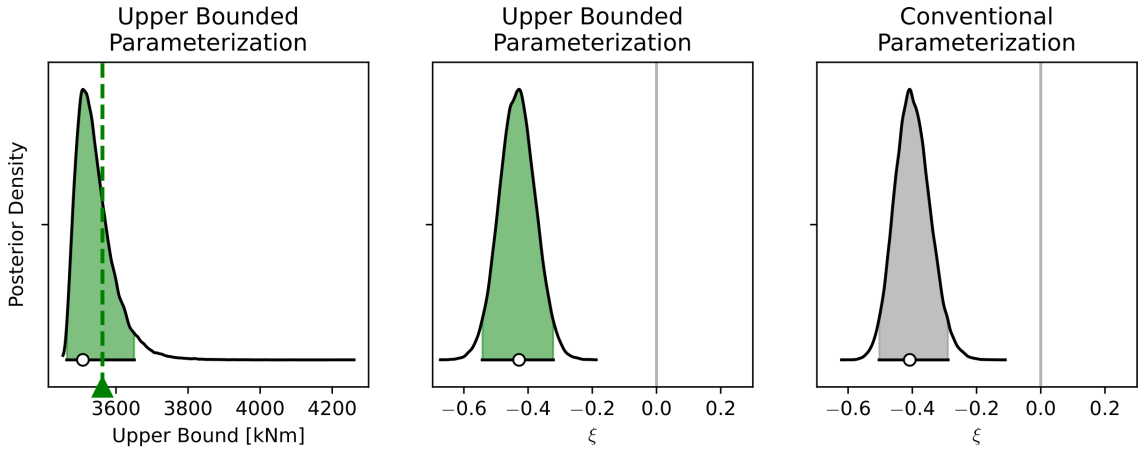


**Figure 5**: Upper bound and $\xi$ parameter posterior distribution fitted to annual maximum traffic load. Green are posterior estimates from the upper-bounded model. Grey is the posterior estimate from the conventional model.

where $X_k$ is the characteristic value of the dimensionless random variable, equal to $1/\lambda_X$, and $\lambda_X$ is the bias of the variable $X$ (Table 1).

The dimensionless limit state function allows the analysis of all structures with varying self-weight, superimposed, and live load by varying $a_g$ and $a_q$ within the range of $0$ and $1$ [3].

| Random Variable | Symbol | Distribution | Bias | CoV | $\xi$ | Reference(s) |
|---|---|---|---|---|---|---|
| Resistance Model Error | $\omega_R$ | Normal | 1.06 | 0.05 | - | [24] |
| Loading Model Error | $\omega_S$ | Log-Normal | 1.00 | 0.10 | - | [11] |
| Resistance | $R$ | Normal | 1.08 | 0.03 | - | [25] |
| Self-weight Load | $G$ | Normal | 1.08 | 0.08 | - | [26] |
| Permanent Load | $P$ | Normal | 1.08 | 0.25 | - | [26] |
| Live Load | $Q$ | GEV | 0.50 | Varies | Varies | [11, 1, 4] |

**Table 1**: Probability models for the reliability analysis.

### 4.2 Physical Consistency in the Live Load Model

The live load distribution is commonly modelled using the unbounded Gumbel distribution, which has a non-zero probability of loading beyond what is physically possible. This leads to a physically inconsistent model, where it is possible to obtain a design point (i.e., the point of most likely failure) beyond what is physically possible (Figure 6). This results in an overestimation of failure probability, as impossible traffic load is computed as the one most likely to cause failure. The use of a correctly upper-bounded distribution avoids this issue by assigning zero probability on all values beyond the estimated upper bound.

### 4.3 Parametric Comparison

To explore the implications of using a physically consistent live load model (i.e., upper-bounded), reliability analysis is performed over the range of dead and live load proportions ($a_g$ and $a_q$), the live load uncertainty (coefficient of variation), and the “upper-boundedness” of the live load as measured by the GEV $\xi$ parameter. Note that the more negative $\xi$ suggests an upper bound closer to the mean,

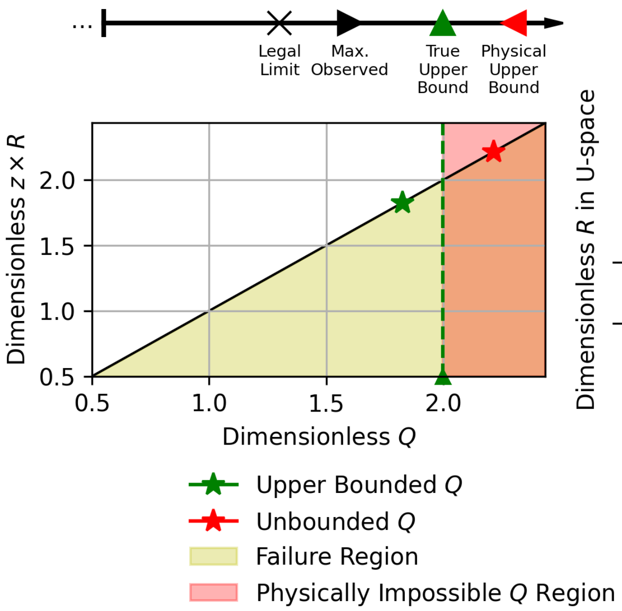


**Figure 6**: Design point of the upper-bounded and conventional (unbounded) live load model. The left plot is in the dimensionless physical space. The right plot is in the standard normal space (U-space). Notice that the unbounded model design point falls in a physically impossible region (larger than the upper bound of the live load).

while $\xi$ closer to zero indicates an upper bound closer to infinity. The reliability index is obtained using the first-order reliability method and verified using the second-order reliability method [27, 28].

Figure 7 shows the reliability index obtained using the conventional Gumbel distribution, physically consistent (upper-bounded) model with varying $\xi$, and heavy-tailed (Fréchet) live load model. The reliability indices obtained using the physically bounded model are higher than those obtained using the conventional unbounded live load model, in line with Section 4.2. This reveals safety reserves in existing probabilistic (and semi-probabilistic) codes and standards using the conventional live load model, leading to potential efficiency improvement without compromising safety in the next generation of codes and standards.

## 5 CONCLUSIONS

In this work, we have shown that traffic (live) loading is an upper-bounded process, and we propose a method to estimate its upper bound. The use of an upper-bounded live load model avoids physically impossible values, leading to a physically consistent model. Future studies should carefully consider the underlying physical processes when choosing a statistical distribution to model physical processes, such as bridge traffic loading. Finally, the use of a physically consistent live load model reveals hidden safety that exists in common reliability analysis using unbounded live load models, which could be exploited by future works to improve efficiency by removing undue conservatism in relevant codes and standards.

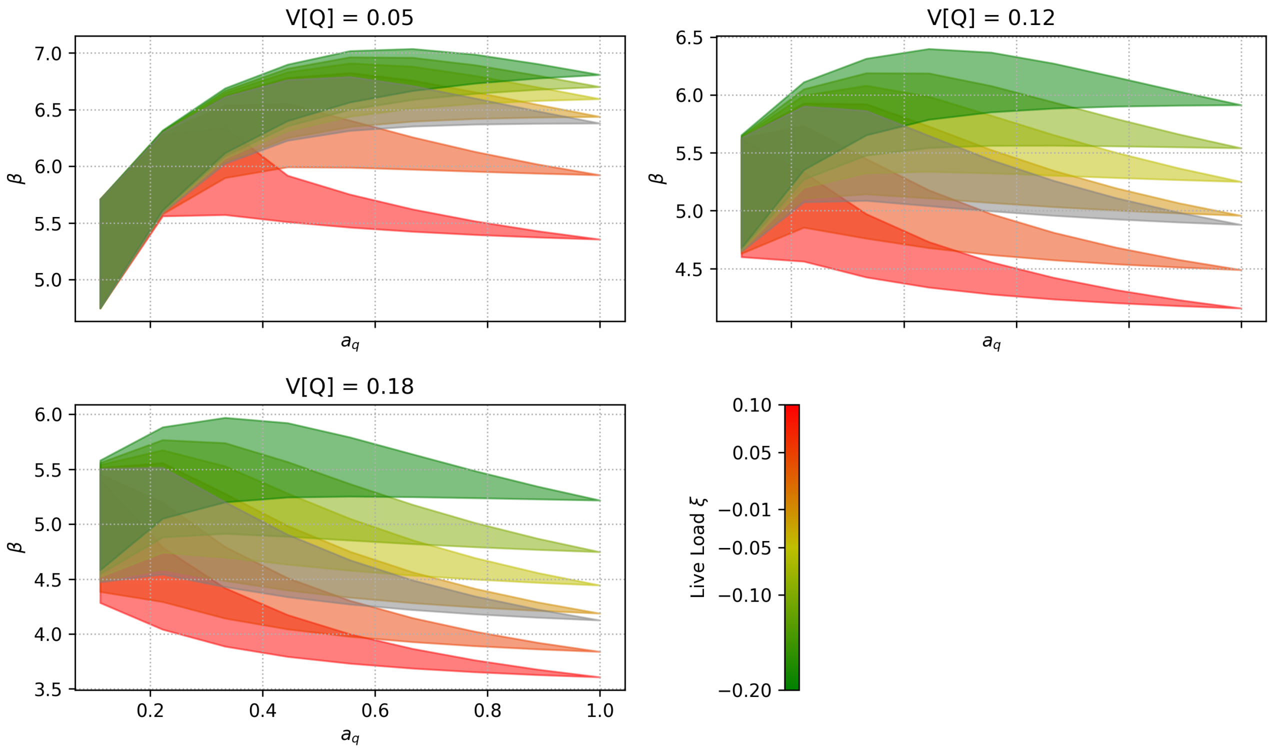


**Figure 7**: Reliability indices ($\beta$) of structures across different self weight ratio ($a_g$), live load ratio ($a_q$), live load coefficient of variation ($V[Q]$), and live load upper boundedness ($\xi$). The yellow to green bands are obtained from bounded traffic load models ($\xi < 0$). The grey bands are obtained from the conventional unbounded (Gumbel) model ($\xi = 0$). The orange to red bands are obtained from heavy-tailed (Fréchet) models ($\xi > 0$).

## REFERENCES


[1] E. J. O'Brien, A. S. Nowak, C. C. Caprani, Bridge Traffic Loading: From Research to Practice, 1st Edition, CRC Press, 2021.

[2] M. M. Melhem, C. C. Caprani, M. G. Stewart, Reliability updating of partial factors for empirical codes: Application to Super-T PSC girders designs at the ultimate limit state in bending, Structures 35 (2022) 233–242. doi:10.1016/j.istruc.2021.11.008.

[3] C. Caprani, M. S. Khan, J. W. Ngan, Probabilistic Design of Standardised U-Trough Bridge Girders for the Victorian Broad Gauge Network, Tech. rep., Monash University, artwork Size: 17792258 Bytes (2024). doi:10.26180/28033280.

[4] M. M. Melhem, C. C. Caprani, M. G. Stewart, S. Zhang, Bridge Assessment Beyond the AS 5100 Deterministic Methodology, Research Project AP-R617-20, Austroads, Australia (Mar. 2020).

[5] C. C. Caprani, Probabilistic Analysis of Highway Bridge Traffic Loading, Ph.D. thesis, University College Dublin, Dublin, Ireland (Oct. 2005).

[6] P. van der Spuy, P. Francois, Derivation of a traffic load model for the structural design of highway bridges in South Africa, Thesis, Stellenbosch : Stellenbosch University, accepted: 2020-02-05T12:41:02Z (Mar. 2020).

[7] C. C. Caprani, E. J. OBrien, G. J. McLachlan, Characteristic traffic load effects from a mixture of loading events on short to medium span bridges, Structural Safety 30 (5) (2008) 394–404. doi:10.1016/j.strusafe.2006.11.006.

[8] B. Dai, Y. Xia, Q. Li, An extreme value prediction method based on clustering algorithm, Reliability Engineering & System Safety 222 (2022) 108442. doi:10.1016/j.ress.2022.108442.

[9] A. Rizqiansyah, C. C. Caprani, Hierarchical Bayesian modeling of highway bridge network extreme traffic loading, Structural Safety 111 (2024) 102503. doi:10.1016/j.strusafe.2024.102503.

[10] Y. Yu, C. S. Cai, Prediction of Extreme Traffic Load Effects of Bridges Using Bayesian Method and Application to Bridge Condition Assessment, Journal of Bridge Engineering 24 (3) (2019) 04019003, publisher: American Society of Civil Engineers. doi:10.1061/(ASCE)BE.1943-5592.0001357.

[11] Joint Committee on Structural Safety, JCSS Probabilistic Model Code, 2000.

[12] S. Coles, An introduction to statistical modeling of extreme values, Springer series in statistics, Springer, London ; New York, 2001.

[13] M. D. Hoffman, A. Gelman, The No-U-Turn Sampler: Adaptively Setting Path Lengths in Hamiltonian Monte Carlo (Apr. 2014).

[14] J. Salvatier, T. V. Wiecki, C. Fonnesbeck, Probabilistic programming in Python using PyMC3, PeerJ Computer Science 2 (2016) e55, publisher: PeerJ Inc. doi:10.7717/peerj-cs.55.

[15] D. R. Heywood, T. Ellis, The Austroads bridge live load model proposal for discussion (1997).

[16] R. Pearson, C. Bayley, Economic Impacts of Higher Bridge Design Loadings, Stage I: Vehicle Alternative and Benefits, Tech. Rep. RUM.H.96, AUSTROADS (1997).

[17] R. Gordon, G. Boully, Revised Bridge Design Live Load, Sydney, New South Wales, Australia, 1997.

[18] J. Galambos, The asymptotic theory of extreme order statistics, 2nd Edition, Krieger, Malabar, Fla, 1987.

[19] J. van Rooyen, A Regional Characterisation and Calibration of Load Effects for Normal and Abnormal Vehicles for the Structural Design of Highway Bridges in South Africa (2023).

[20] M. Falk, F. Marohn, Von Mises Conditions Revisited, The Annals of Probability 21 (3) (Jul. 1993). doi:10.1214/aop/1176989120.

[21] Z. Zhou, C. Caprani, PyBTLS: A Python package for traffic load simulation on short-to-medium bridges, in: Bridge Maintenance, Safety, Management, Digitalization and Sustainability, CRC Press, Copenhagen, Denmark, 2024.

[22] J. Köhler, R. Hingorani, J. D. Sørensen, Reliability Level of the Second Generation of the Eurocodes – Status and Potential, Dublin, Ireland, 2023.

[23] J. Köhler, J. D. Sørensen, B. Ellingwood, Codes and standards for structural design - developments and future potential, Structural Safety 113 (2025) 102495. doi:10.1016/j.strusafe.2024.102495.

[24] S. J. Foster, M. G. Stewart, M. Loo, M. Ahammed, V. Sirivivatnanon, Calibration of Australian Standard AS3600 Concrete Structures: part I statistical analysis of material properties and model error, Australian Journal of Structural Engineering 17 (4) (2016) 242–253. doi:10.1080/13287982.2016.1246793.

[25] M. Melhem, C. Caprani, M. Stewart, A. Ng, Bridge safety assessment beyond deterministic methods: An Australian perspective, in: H. Yokota, D. M. Frangopol (Eds.), Bridge Maintenance, Safety, Management, Life-Cycle Sustainability and Innovations, 1st Edition, CRC Press, 2021, pp. 551–559. doi:10.1201/9780429279119-72.
URL https://www.taylorfrancis.com/books/9781000173758/chapters/10.1201/9780429279119-72

[26] A. M. Rakoczy, A. S. Nowak, Reliability-based sensitivity analysis for prestressed concrete girder bridges, PCI Journal 58 (4) (2013) 81–92. doi:10.15554/pcij.09012013.81.92.

[27] A. M. Hasofer, N. C. Lind, An exact invariant first order reliability format 100 (1974) 111–121.

[28] H. O. Madsen, S. Krenk, N. C. Lind, Methods of Structural Safety, Prentice Hal, Inc., Englewood Cliffs, NJ, 2006.